



PERGAMON

Atmospheric Environment 35 (2001) 2845–2860

**ATMOSPHERIC
ENVIRONMENT**

www.elsevier.com/locate/atmosenv

Estimates of aerosol species scattering characteristics as a function of relative humidity

William C. Malm*, Derek E. Day

National Park Service-Air Resources, CIRA/Colorado State University, Fort Collins, CO 80523, USA

Received 11 April 2000; received in revised form 18 December 2000; accepted 21 December 2000

Abstract

The absorption of water by ambient aerosols can significantly increase the light scattering coefficient and thereby affect issues such as visibility and climate forcing. Although water absorption by inorganic compounds and mixtures of inorganic compounds can often be modeled with adequate certainty for most applications, modeling water uptake by organic aerosols at present is speculative. In this paper, we present data in the form of $f(\text{RH}) = b_{\text{scat}}(\text{RH})/b_{\text{scat,dry}}$, where $b_{\text{scat}}(\text{RH})$ is the scattering coefficient measured at some relative humidity (RH) > 20% and $b_{\text{scat,dry}}$ is the scattering coefficient measured at RH < 20%. The $f(\text{RH})$ has been measured at Great Smoky Mountains National Park in Tennessee and at Grand Canyon National Park in Arizona. The $f(\text{RH})$ curves obtained from these two sites, which show distinctly different aerosol composition and average RH values, are compared. We also present comparisons between the measured water uptake by ambient aerosol with modeled water uptake by inorganic compounds to estimate the water uptake by organic aerosol. © 2001 Elsevier Science Ltd. All rights reserved.

Keywords: Aerosol; Scattering; Relative humidity

1. Introduction

The ability of atmospheric particulate matter to absorb water can be a significant factor in determining both the extinction cross-section and the total aerosol mass, therefore, water absorption significantly influences visibility and radiative forcing. For instance, at 90% relative humidity (RH), the scattering cross-section of an ammonium sulfate particle can be increased by a factor of five or more above that of the dry particle. The behavior of inorganic salts under variable relative humidity conditions is well established from laboratory experiments. It is known that initially dry inorganic salts exhibit deliquescent properties when exposed to moist atmospheres, but they crystallize under quite different relative humidity conditions (hysteresis behavior) (Tang, 1976; Tang and Munkelwitz, 1991). Laboratory studies of pure inor-

ganic salts (Tang and Munkelwitz, 1994) and of some mixtures of salts (Tang, 1997) have determined their hygroscopic growth and refractive indices as functions of relative humidity. Moreover, droplet growth and its consequences on light extinction can be estimated for both pure and mixed-solute particles solely on the basis of chemical equilibrium equations, together with mass concentrations and applied ion balances (Stelson and Seinfeld, 1982; Pilinis and Seinfeld, 1987; Wexler and Seinfeld, 1991). Quinn and Coffman (1998), among others, have shown the applicability of this thermodynamic approach to estimating light scattering in clean marine regions where ionic species dominate the aerosol chemical composition.

In contrast, the affinities of organic compounds for water, particularly for those species found in the ambient atmosphere, are not as well characterized, despite the fact they often account for a significant amount of the total fine mass in continental aerosols (Malm et al., 1994). As reviewed by Saxena and Hildemann (1996), organic particulate matter contains hundreds of compounds, spanning a range of carbon numbers, functional groups, and

* Corresponding author. Tel.: +1-970-491-8292; fax: +1-970-491-8598.

E-mail address: malm@cira.colostate.edu (W.C. Malm).

solubility in polar and nonpolar solvents. These authors point out, that for several reasons, early work in organic analyses of particulate matter focused on extractions with nonpolar solvents, and thus information on the more polar and presumably more water-soluble components is lacking. Rogge et al. (1993) performed such extractions and subsequent derivatizations for samples collected in Southern California and constructed a mass balance that illustrates some of the difficulties associated with organic species identification. In their work, organic compounds accounted for 13–27% of the fine mass. Only 45–60% of the organic mass was extractable and elutable using their protocols, and only 23–29% of the elutable mass could be resolved. Thus identification of the molecular composition was possible for only a relatively small fraction of the organic mass. Some investigators have determined the fraction of the organic mass extractable in water and compared this with what was extracted in nonpolar solvents. Several such studies were summarized by Saxena and Hildemann (1996) and showed that while nonpolar extractions do recover some water-soluble species, they do not extract all of them. The utility of different approaches was demonstrated recently by Blando et al. (1998) and Decesari et al. (2000). Blando et al. (1998) analyzed samples by Fourier transform infrared (FTIR) spectroscopy, before and after rinsing with polar and nonpolar solvents, to obtain information on functional groups and polarity. They found that the submicron aerosol samples were composed primarily of polar compounds. Decesari et al. (2000) combined chromatographic separations, functional group analyses via different techniques, and total organic carbon analysis to obtain information on a substantial fraction (> 70%) of the water-soluble organic carbon mass.

Rather than attempting to identify specific compounds that may be hygroscopic, some workers have explicitly measured water uptake of organic material emitted by various source types. For instance, McDow et al. (1994) measured water uptake by diesel soot, automobile exhaust, and wood smoke particles. They found that all three emission types absorbed water with the wood smoke sample weight increasing by about 10% as sample relative humidity increased from 40% to 90%. Over the same range of relative humidities, diesel soot sample weight increased by only 2–3%. Chughtai et al. (1999) examined the hydration characteristics of BP2000 (commercially available carbon black), *n*-hexane, diesel, JP8 (aviation fuel), pine needle, Utah coal, and acetylene. They examined water adsorption isotherms between 20% and 85% relative humidity. They concluded the ability of black carbons, produced from a variety of fuel types, to adsorb water generally increased with age and surface oxidation. At high relative humidity (83%), large surface areas determine the adsorption capacity. At lower relative humidity, however, the surface functional groups determine the extent of hydration. Even at 83% relative

humidity, the water uptake was less than 10% of total mass for all carbon species other than BP2000. Because of its large surface area, BP2000 absorbed about 40% of its mass in water. Consequently, they concluded that commercial carbon blacks are not acceptable models for fuel-produced carbons.

Other workers have experimentally measured growth of ambient particles as a function of relative humidity using tandem differential mobility analyzers (TDMA) (Zhang et al., 1993, 1994). One study was carried out at Meadview, Arizona (west end of Grand Canyon) over a 31-day period during the summer of 1991, a second at Hopi Point, Arizona (midpoint of Grand Canyon), a 13-day period during the winter of 1990, while a third was implemented at Claremont, California over an 11-day period during the summer of 1987 (Cai et al., 1993; Zhang et al., 1993, 1994; McMurry and Zhang, 1991). A TDMA consists of two DMAs operated in series. The first DMA is used to select a size, while the second is used to measure the change in particle size as relative humidity is varied. Usually, a MOUDI size sampler (Marple et al., 1991) is run concurrent with the TDMA to derive estimates of particle composition.

At Grand Canyon, the particles are generally grouped into two categories: more hygroscopic containing sulfates, nitrates, and some carbon, and less hygroscopic containing carbon mass not accounted for by the number fraction of the more hygroscopic particles. They also found that some particles deliquesced in the mid 60% relative humidity range while most particles deliquesced at the mid-to-upper 70% relative humidities. Pitchford and McMurry (1994) also report that about 20% of the particles had relatively little growth at any relative humidity.

Saxena et al. (1995), based on their modeling assumptions, concluded that at Grand Canyon organics add to water absorption by inorganics, while at Claremont the net effect of organics is to diminish water absorption by inorganics. On the other hand, Pitchford and McMurry (1994) showed that on 6 of the 8 sampling days at Grand Canyon, if it is assumed that nitrates and sulfates uptake water at the same rate as measured in the laboratory, they alone could account for all of the measured water absorption.

Other studies, originally initiated by Covert et al. (1979) examined the scattering characteristics of ambient aerosols as a function of relative humidity. One nephelometer was operated at 30% relative humidity, while a second at variable relative humidity. They made limited measurements $f(\text{RH}) = b_{\text{wet}}/b_{\text{dry}}$ at Tyson, Missouri and Point Reyes, California. The instrumentation was modified and additional measurements of $b_{\text{wet}}/b_{\text{dry}}$ were made in rural Virginia at Shenandoah National Park and University of Houston, Texas (Waggoner et al., 1983). Humidity was controlled by first diluting sample air with dry air and then humidifying with a variable amount

of water vapor. They also operated a heater and cooler in series with the humidifier (thermidograph), which allowed them to infer compositional structure of the aerosol.

They were able to dry the aerosol to about 30% RH and their first $f(\text{RH})$ data points start at about 35%. The singular most interesting feature of their $f(\text{RH})$ curves for Shenandoah is that they appear to be continuous over the range of RH values that they measured; that is, they did not show evidence of supersaturation. On the other hand, at Houston, Texas, they concluded that the particles were supersaturated about one-third of the time. The range of $f(\text{RH})$ values at 90% RH varied from a low of about 1.5 to a high of about 2.2–2.6. Moreover, at Shenandoah, the thermogram measurement allowed them to extract only sulfate scattering at 65–70% RH, and it was their conclusion that at 70% RH all the water, within the uncertainty of their measurements, is associated with the ammonium plus sulfate fraction of fine particle mass.

Understanding the hygroscopic properties of ambient aerosols was, in part, the motivation for the two field studies reported on in this paper. The inability to conclusively apportion about 30–50% of the extinction budget between coarse mass scattering and particle absorption at many of our national parks was also an important motivating factor.

To address these issues, two studies were carried out, one in the eastern United States at Great Smoky Mountains and the other at Grand Canyon National Park. The Southeastern Aerosol and Visibility Study (SEAVS) was conducted from 15 July 1995 through 25 August 1995 in Great Smoky Mountains National Park. The study was a collaborative effort between several universities, consulting firms, the Electric Power Research Institute (EPRI), and the National Park Service (NPS). The Grand Canyon study was carried out from 10 July 1998 through 8 August 1998 on the south rim of Grand Canyon National Park. The overall objectives of the studies were to better understand the physical, chemical, and optical characteristics of the ambient aerosol in the humid southeastern United States on the one hand and the relatively dry conditions observed on the Colorado Plateau during the summer months on the other.

Experiments were designed such that observables could be estimated or modeled in a number of different ways. Fine mass was gravimetrically determined for both PM₁₀ and PM_{2.5}, which can be compared to reconstructed mass based on measured species. Dry and ambient 2.5 μm scattering was measured, which in turn can be compared to reconstructed scattering based on aerosol species measurements. Nephelometry was used to measure ambient scattering of fine and coarse particles, which in turn can be used with extinction measurements to develop estimates of absorption. Fine and coarse mass absorption was also derived from transmission measure-

ments on two types of filter substrates and, in addition, fine mass absorption was measured with an aethalometer. Light scattering (b_{scat}) measured as a function of relative humidity ($f(\text{RH}) = b_{\text{scat}(\text{wet})}/b_{\text{scat}(\text{dry})}$) is compared to modeled aerosol growth. Comparing the modeled light scattering with measured light scattering and comparing modeled wet-to-dry scattering ratios with measured ratios will serve to both explore the validity of aerosol growth models, mixing models and associated assumptions and provide an estimate of the hygroscopicity of aerosol species other than sulfates and nitrates.

This paper will focus on the qualitative and quantitative aspects of measured $f(\text{RH})$ curves as a function of aerosol species concentrations. A statistical technique to estimate the aerosol growth of individual species is presented and results from the two studies are compared.

2. Measurements

2.1. Humidograph

The hygroscopic properties of ambient particles are examined using a humidograph with the ability to measure scattering as a function of humidity over ranges of about 15–95%. Day et al. (2000) describe the instrument design in some detail and therefore its operation will only be summarized here.

Air is drawn through a temperature moderated humidity conditioner and passed into a Radiance Research M903 integrating nephelometer. The humidity conditioner consists of an array of Perma Pure Nafion drying tubes. The tubes are housed in a water bath, which moderates temperature changes in the sample aerosol. Sample RH and temperature are monitored throughout the system.

2.2. Integrating nephelometers

The details of ambient nephelometer measurements and their uncertainties are covered in Malm et al. (1994) and Day et al. (1997) and therefore will only be briefly reviewed here. Optec NGN-2 integrating nephelometers, in various configurations, were operated during both studies and in a redundant fashion to establish the precision of the measurements. The nephelometers were operated in the open-air configuration according to standard IMPROVE protocols (Molenaar, 1997; Malm et al., 1994) and with a Bendix-240 (Chan and Lippman, 1977) cyclone inlet, with a 2.5 μm cutpoint.

2.3. Relative humidity sensors

Three Rotronics mp 100f combination relative humidity/temperature sensors were housed in PVC holders and aspirated by a fan. The flow rate through the holder was

approximately 120 l min^{-1} . The sensors were approximately 6 feet above ground level, 6 feet from each other, and mounted near the inlets of the nephelometers.

2.4. Particulate samplers

The IMPROVE sampler was designed for the IMPROVE network and has been operated extensively in the network and during field studies since 1988 (Malm et al., 1994). The IMPROVE sampler consists of four independent modules. Each module incorporates a separate inlet array, filter pack, and pump assembly, however, all modules are controlled by the same singular timing mechanism. It is convenient to consider a particular module, its associated filter, and the parameters measured from the filter as a channel of measurement (i.e., channel A). Channels A, B, and C are equipped with a $2.5 \mu\text{m}$ cyclone. The channel A Teflon filter is analyzed for fine mass (PM_{2.5}) gravimetrically, nearly all elements with atomic mass number > 11 (which is Na) and < 82 (which is Pb) by proton induced X-ray emission (PIXE) and by X-ray fluorescence (XRF), elemental hydrogen by proton elastic scattering analysis (PESA), and for light absorption.

Channel B utilizes a single Nylasorb filter as a collection substrate. The material collected from the filter is extracted ultrasonically in an aqueous solution that is subsequently analyzed by ion chromatography for the anions sulfate, nitrate, nitrite and chloride. At the Great Smoky site, the ammonium ion concentration was also measured using extracts from these filters in a separate colorimetric analysis.

Channel C utilizes tandem quartz fiber filters for the collection of fine particles, and the estimation of the organic carbon artifact from organic gases collected on the secondary filter. These filters are analyzed by thermal optical reflectance (TOR) for elemental and organic carbon (Chow et al., 1993).

Channel D, fitted with a PM₁₀ inlet, utilizes a Teflon filter, which is gravimetrically analyzed for mass (PM₁₀), and at Grand Canyon it was also analyzed for elements using the PIXE and PESA techniques. Exposed cassettes from channels A, B, and D were stored in sealed plastic bags and shipped for storage and analysis, while exposed sample cassettes from channel C were stored in a freezer for the duration of the study. The channel C carbon filters were packed in a cooler and shipped on ice for analysis.

At the Great Smoky site, mass size distributions were measured using the DRUM sampler (Cahill et al., 1985), an eight stage, single orifice cascade impactor. The accelerating orifices result in size cuts at 10.0, 5.0, 2.5, 1.15, 0.56, 0.34, 0.24 and $0.07 \mu\text{m}$ aerodynamic diameter. A backup filter collects particles below $0.07 \mu\text{m}$, but normally without resolution in time. Particle loss through the first five stages ($< 2.5 \mu\text{m}$) was measured at 9%

(Raabe et al., 1988; Chow et al., 1993), while particle bounce associated with dry soil aerosols is under one part in 5000 by mass (Cahill et al., 1985).

3. Determination of aerosol species mass

Most fine sulfates are the result of oxidation of SO_2 gas to sulfate particles. In humid atmospheres, the oxidation typically occurs in clouds where sulfuric acid is formed within water droplets. If there is inadequate ammonia in the atmosphere to fully neutralize the sulfuric acid, as is sometimes the case, then the resulting aerosols are acidic. Under these circumstances solutions of continuously varying acidity are formed. The extremes of this continuum are ammonium sulfate (neutral) and sulfuric acid. The dry ammoniated sulfate concentration is calculated from measured SO_4 and NH_4 ions using:

$$[\text{SO}_{4,\text{mass}}] = (0.944)[\text{NH}_4^+] + (1.02)[\text{SO}_4^{2-}], \quad (1)$$

where $[\text{SO}_{4,\text{mass}}]$ is the concentration of the ammoniated sulfate, $[\text{SO}_4^{2-}]$ is the concentration of sulfate ion and $[\text{NH}_4^+]$ is the concentration of ammonium ion after adjusting for the ammonium associated with ammonium nitrate. If only the sulfate ion is measured, one must assume a form of sulfate and multiply by an appropriate multiplication factor, for instance, 1.37SO_4 , if ammonium sulfate is assumed.

An average ambient particulate organic compound is assumed to have a constant fraction of carbon by weight. Organic carbon mass (OMC) is therefore estimated using:

$$[\text{OMC}] = (1.4)[\text{OC}]. \quad (2)$$

The factor of 1.4 corrects the organic carbon mass for other elements associated with the organic carbon molecule (Watson et al., 1988).

Organic mass can also be estimated from the concentrations of H and S measured on the channel A Teflon filter if certain assumptions are made (Malm et al., 1994). It is assumed that during exposure to the vacuum of channel A PIXE and PESA analyses, all nitrates and water volatilize and do not contribute to the mass of H. It is further assumed that the remaining hydrogen can be apportioned between sulfates and organic carbon. For instance, assuming full neutralization of the sulfate ion, organic carbon by hydrogen (OCH) is calculated using

$$[\text{OCH}] = 11([\text{H}] - 0.25[\text{S}]). \quad (3)$$

The sulfur factors derived from the H/S ratio for ammonium sulfate are $8/32$ or 0.25 . The C/H ratio is 11 and operationally defined by forcing OC to equal OCH. Comparison of OCH to OC is used in data validation procedures and OCH is used to estimate organic mass

Table 1

Statistical summary of aerosol species concentrations and the fraction of reconstructed fine mass attributed to certain species from Great Smoky. FM, RECON, Ammoniated Sulfate, NH_4NO_3 , OMC, EC, SOIL, CM, and NH_4 are gravimetric fine mass, reconstructed fine mass, sulfate plus ammonium mass, ammonium nitrate, organic, and elemental carbon, soil, coarse mass, and ammonium ion mass

Variable	Mean ($\mu\text{g m}^{-3}$)	SD ($\mu\text{g m}^{-3}$)	Minimum ($\mu\text{g m}^{-3}$)	Maximum ($\mu\text{g m}^{-3}$)	Fraction	N
FM	25.13	17.55	0.00	87.94	1.38	80
RECON	18.09	12.34	3.66	59.41	1.00	80
Ammoniated sulfate	11.42	10.32	1.17	48.23	0.63	80
NH_4NO_3	0.20	0.11	0.07	0.70	0.01	80
OMC	4.56	1.80	1.40	8.61	0.25	80
EC	0.44	0.25	0.00	1.17	0.02	80
SOIL	1.47	1.56	0.02	8.33	0.08	80
CM	6.16	5.85	0.00	24.69	NA	80
NH_4	1.79	1.30	0.06	4.98	NA	80
NH_4/SO_4 Molar ratio	1.10	0.30	0.30	1.85	NA	80

Table 2

Statistical summary of aerosol species concentrations and the fraction of reconstructed fine mass attributed to certain species from Grand Canyon. FM, RECON, $(\text{NH}_4)_2\text{SO}_4$, NH_4NO_3 , OMC, OMH, EC, SOIL, and CM are gravimetric fine mass, reconstructed fine mass, ammonium sulfate, ammonium nitrate, organics by TOR, organics by hydrogen, elemental carbon, soil and coarse mass

Variable	Mean ($\mu\text{g m}^{-3}$)	SD ($\mu\text{g m}^{-3}$)	Minimum ($\mu\text{g m}^{-3}$)	Maximum ($\mu\text{g m}^{-3}$)	Fraction	N
FM	3.92	1.50	1.46	8.78	NA	51
RECON	3.71	1.51	1.34	9.34	1.00	51
$(\text{NH}_4)_2\text{SO}_4$	1.17	0.66	0.28	3.01	0.31	51
NH_4NO_3	0.19	0.12	0.03	0.55	0.05	51
OMC	1.62	1.15	0.21	7.05	0.44	51
OMH	1.62	0.69	0.85	4.44	0.44	51
EC	0.11	0.14	-0.04	0.69	0.03	51
SOIL	0.62	0.25	0.25	1.28	0.17	51
CM	4.61	7.25	0.00	50.32	NA	51

when carbon is not explicitly measured (Malm et al., 1994).

Assuming the measured nitrate ion is associated with the ammonium ion as (NH_4NO_3) , the nitrate compound mass is estimated from the nitrate ion mass concentration by using a multiplication factor of 1.29.

Soil mass concentration is estimated by summing the elements predominantly associated with soil, plus oxygen for the common compounds (Al_2O_3 , SiO_2 , CaO , K_2O , FeO , Fe_2O_3 , TiO_2), plus a correction for other compounds such as MgO , Na_2O , water, and carbonate.

The sum of these five constituents, plus water, provides a reasonable estimate of the fine mass measured on the Teflon filter. However, a significant fraction of the nitrate particulate mass can volatilize from the Teflon filter during collection and is not measured by gravimetric analysis (Zhang and McMurry, 1992).

4. Summary of aerosol measurements and their optical characteristics

A discussion of aerosol data and its optical properties collected at Great Smoky is presented in Malm et al. (2000) and those collected at Grand Canyon in Malm and Day (2000). However, an abbreviated summary of the aerosol measurements will be presented here for completeness and for purposes of putting the calculations presented in this paper in a better perspective. Tables 1 and 2 present a statistical summary of aerosol species concentrations. At Grand Canyon, it was assumed that the molecular form of sulfate was ammonium sulfate.

There are some striking differences in aerosol concentration between the two national parks. The average fine mass at Great Smoky is $25 \mu\text{g m}^{-3}$ with a maximum near $90 \mu\text{g m}^{-3}$, while at Grand Canyon the average is

$3.9 \mu\text{g m}^{-3}$ with a maximum of only $8.8 \mu\text{g m}^{-3}$. Of the $90 \mu\text{g m}^{-3}$ fine mass concentration $48 \mu\text{g m}^{-3}$ was ammoniated sulfate. On the average, at Great Smoky sulfates plus ammonium comprise 63% of the fine mass, while at Grand Canyon they are 31%. At Grand Canyon, organics are the largest fraction of fine mass at 44%. Also at Grand Canyon, the maximum coarse mass concentration was $50 \mu\text{g m}^{-3}$, while at Great Smoky it was only $25 \mu\text{g m}^{-3}$. At both parks, ammonium nitrate and elemental carbon are less than 5% of the fine mass, however, at Great Smoky fine soil is also low at 8%, while at Grand Canyon it is 17%.

At Grand Canyon, the composition of coarse mass was unexpected in that organic mass concentrations were comparable to soil/dust, and there were many days when coarse organics were the largest fraction of coarse mass. On the other hand, one coarse mass episode had a 24 h dust concentration of $17.99 \mu\text{g m}^{-3}$ with a $3.65 \mu\text{g m}^{-3}$ organic mass concentration. Coarse sulfates were less than 1–2% of coarse mass.

4.1. Comparison between estimated and measured scattering at Great Smoky Mountains National Park

Malm et al. (2000) examined the ability of various models to predict scattering of fine particles less than $2.5 \mu\text{m}$ using the Great Smoky data set. In the following discussion, external mixture refers to the assumption that the measured species are not mixed with each other. That is sulfate particles are physically separate from organic particles, which in turn are separate from nitrate particles. The reference to internal model refers to the assumption that sulfates, nitrates, and organics are all mixed uniformly with each other, but soil is externally mixed to sulfate, nitrates, and organics.

Two external models were assumed, one with constant sulfate ammoniation (ammonium bisulfate) and constant dry mass scattering efficiencies. In the second, sulfate mass and growth as a function of relative humidity was accounted for as a function of sulfate ammoniation. The assumed nominal values for dry mass scattering efficiencies for sulfates and nitrates were $3.0 \text{ m}^2 \text{ gm}^{-1}$. Organics and fine soil were 4.0 and $1.0 \text{ m}^2 \text{ gm}^{-1}$, respectively (Malm et al., 1994; Trijonis et al., 1990). Third, an externally mixed aerosol model, where sulfate mass scattering efficiencies as a function of sulfate mass size distributions and ammoniation, was incorporated, and finally, an internally mixed aerosol model that included sulfate size, ammoniation, and associated sulfate growth was exercised. Size distributions for nitrates and organics were assumed to have the same size distribution as sulfur. In all cases, only sulfate and nitrate were considered to be hygroscopic.

When comparing model performance as it relates to predicting ambient scattering, the first and simplest model, which assumed only one type of sulfate species

and constant mass scattering efficiencies, performed the poorest. It predicted ambient scattering adequately at low scattering values, but under predicted scattering under high sulfate concentrations by about 30%. Model performance was improved substantially by estimating absorbed water as a function of sulfate ammoniation. Only slight improvement in model performance was achieved by explicitly accounting for variation in dry mass scattering coefficients due to changes in particle size distribution.

As discussed in Section 1, sulfates and other inorganic salts demonstrate a hysteresis in their growth curves as a function of relative humidity by abruptly absorbing water (deliquesce) at quite a different relative humidity than the relative humidity at which they recrystallize. The effect on estimated scattering associated with assuming the crystallization, deliquescent branches, or the “best estimate”, which consists of smoothing the hysteresis curves between the deliquescent and crystallization points, was also examined and found to be small. Furthermore, the difference between the internal and external assumptions was found to be small. The average difference between the two calculations was only about 8%, with the mixed model yielding the higher reconstructed scattering estimates.

4.2. Comparison between estimated and measured scattering at Grand Canyon National Park

At Grand Canyon, fine mass scattering efficiencies deviated from the nominal values used in the Great Smoky data set. The best match between reconstructed and measured fine particle scattering was achieved using mass scattering efficiencies of 2.2 and $1.8 \text{ m}^2 \text{ gm}^{-1}$ for sulfates and organics, respectively. The sulfate mass scattering efficiency is based on mass size distributions measured at Grand Canyon and discussed in Malm and Pitchford (1997), while the estimate of organic mass scattering efficiency is based on the data collected in summer of 1998 and reported in Malm et al. (2000). Using the nominal value of $4.0 \text{ m}^2 \text{ gm}^{-1}$ for organics resulted in over predicting measured scattering by about 50%. Regression results suggested an organics mass scattering coefficient of 1.8 ± 0.28 as well as verifying that $2.2 \text{ m}^2 \text{ gm}^{-1}$ was about right for sulfates. The finding of a low fine organic mass scattering efficiency is consistent with organics mass size distributions with mass mean diameters of around $2.0 \mu\text{m}$.

5. General features of the $f(\text{RH})=b_{\text{scat}}(\text{RH})/b_{\text{scat,dry}}$ curves

The ratio between dry and wet scattering as a function of RH is referred to as the relative humidity scattering enhancement factor, $f(\text{RH})$. Fig. 1 shows all the $f(\text{RH})$ data points for the Great Smoky data set, while Table

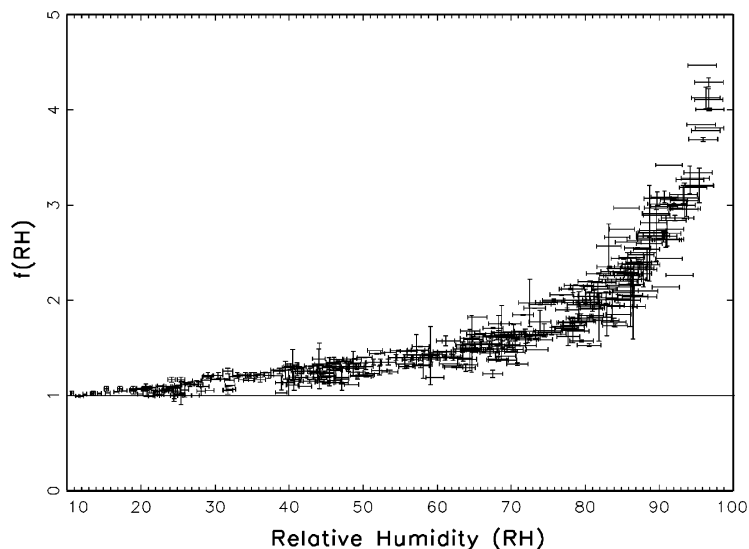


Fig. 1. Scatter plot of all measured $f(\text{RH})$ data points collected during the Great Smoky study.

Table 3

Statistical summary of mean $f(\text{RH})$ values in selected relative humidity ranges for the Great Smoky data set. Also shown are the corresponding theoretical estimates of $f(\text{RH})$

Relative humidity	Mean	SD	Predicted	Minimum	Maximum	<i>N</i>
20 < RH ≤ 25	1.06	0.036	1.01	0.99	1.16	36
25 < RH ≤ 30	1.11	0.07	1.04	1.00	1.21	18
30 < RH ≤ 35	1.16	0.06	1.06	1.05	1.25	17
35 < RH ≤ 40	1.21	0.07	1.09	1.03	1.29	12
40 < RH ≤ 45	1.22	0.08	1.14	1.10	1.38	27
45 < RH ≤ 50	1.27	0.08	1.20	1.11	1.38	29
50 < RH ≤ 55	1.33	0.10	1.27	1.20	1.47	17
55 < RH ≤ 60	1.38	0.08	1.35	1.19	1.51	17
60 < RH ≤ 65	1.45	0.10	1.45	1.29	1.68	26
65 < RH ≤ 70	1.55	0.12	1.58	1.23	1.82	33
70 < RH ≤ 75	1.65	0.17	1.73	1.33	1.98	23
75 < RH ≤ 80	1.83	0.17	1.91	1.57	2.16	31
80 < RH ≤ 85	2.10	0.23	2.12	1.53	2.75	43
85 < RH ≤ 90	2.46	0.29	2.43	1.93	3.07	48
RH > 90	3.17	0.29	3.01	2.14	4.47	40

3 gives a statistical summary of that data. Over the course of the study, ammonium to sulfate molar ratios varied from a low of 0.30 to a high of 1.85 with an average of 1.1 ± 0.30 . Fig. 2a curve similar to Fig. 1, shows the $f(\text{RH})$ data collected at Grand Canyon. Because of the increased number of data points the average of all $f(\text{RH})$ values for a given run and within a given RH range is plotted instead of individual data points. A statistical summary of the data is presented in Table 4.

Although the growth curves did not show “step function” jumps in growth at any relative humidity the onset of growth at some specific relative humidity will be referred to as deliquescence. At Grand Canyon there were 36 sampling days where $f(\text{RH})$ was measured and on 6 days particles deliquesced in the 25–35% RH range, 24 in the 35–45% range, and 6 in the 45–55% RH range. Also interesting is that on 16 of the 36 days when particles deliquesced in the 25–55% RH range, a second discontinuous increase in $f(\text{RH})$ occurred in the 60–70% RH range.

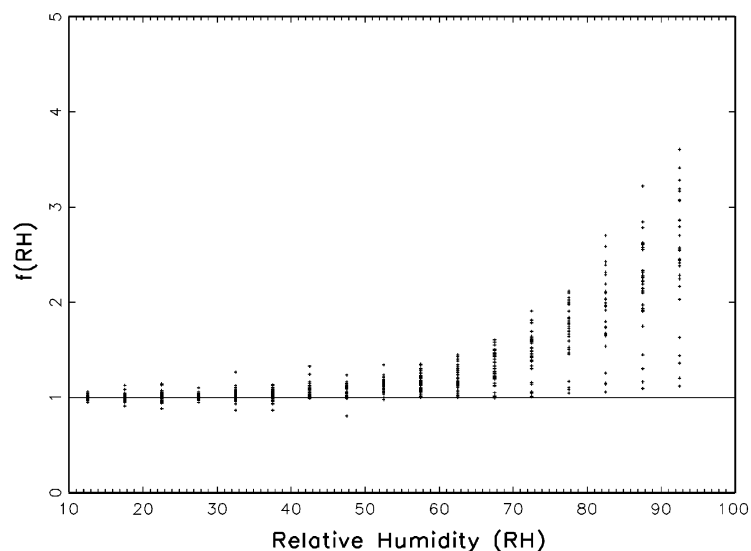


Fig. 2. Scatter plot of measured $f(\text{RH})$ data points that have been averaged into 5% relative humidity “bins” for the Grand Canyon data set. The total number of data points for this data set was approximately 7500.

Table 4

Statistical summary of mean $f(\text{RH})$ values in selected relative humidity ranges for the Grand Canyon data set. Also shown are the corresponding theoretical estimates of $f(\text{RH})$

Relative humidity	Mean	SD	Predicted	Minimum	Maximum	<i>N</i>
15 ≤ RH < 20	0.99	0.08	1.00	0.68	1.47	350
20 ≤ RH < 25	1.00	0.09	1.00	0.68	1.54	195
25 ≤ RH < 30	1.01	0.1	1.00	0.71	1.43	343
30 ≤ RH < 35	1.03	0.11	1.00	0.6	1.39	327
35 ≤ RH < 40	1.05	0.12	1.01	0.65	1.50	319
40 ≤ RH < 45	1.08	0.13	1.06	0.69	2.18	361
45 ≤ RH < 50	1.10	0.13	1.11	0.63	1.66	395
50 ≤ RH < 55	1.15	0.13	1.17	0.74	1.56	493
55 ≤ RH < 60	1.21	0.15	1.24	0.87	1.89	559
60 ≤ RH < 65	1.27	0.18	1.33	0.65	1.82	557
65 ≤ RH < 70	1.36	0.19	1.43	0.83	1.84	829
70 ≤ RH < 75	1.46	0.24	1.55	0.94	2.43	622
75 ≤ RH < 80	1.63	0.32	1.70	0.71	3.58	620
80 ≤ RH < 85	1.92	0.38	1.87	0.94	4.00	725
85 ≤ RH < 90	2.24	0.48	2.14	1.07	4.84	835

Two of the $f(\text{RH})$ curves where there is evidence for two deliquescent points are shown in Fig. 3. Fig. 3 shows “typical” runs for Julian days 204, 212, and 217. The lines through the data points correspond to theoretical predictions of $f(\text{RH})$, which will be discussed in the next section. The curves for Julian day 204 and 212 show little or no growth until about 50% RH where $f(\text{RH})$ increases and stays about the same until about 67% RH. Above 67% RH, the $f(\text{RH})$ abruptly increases again and then in-

creases continually to above 90% RH. On Julian day 204, sulfates and nitrates made up 39% and 7% of the fine mass while on Julian day 212, 48% and 8% of the fine mass was in the form of sulfates and nitrates, respectively.

These findings are consistent with the TDMA measurements made at Grand Canyon reported by Pitchford and McMurry (1994) and by Saxena et al. (1995). Pitchford and McMurry (1994) report that in the

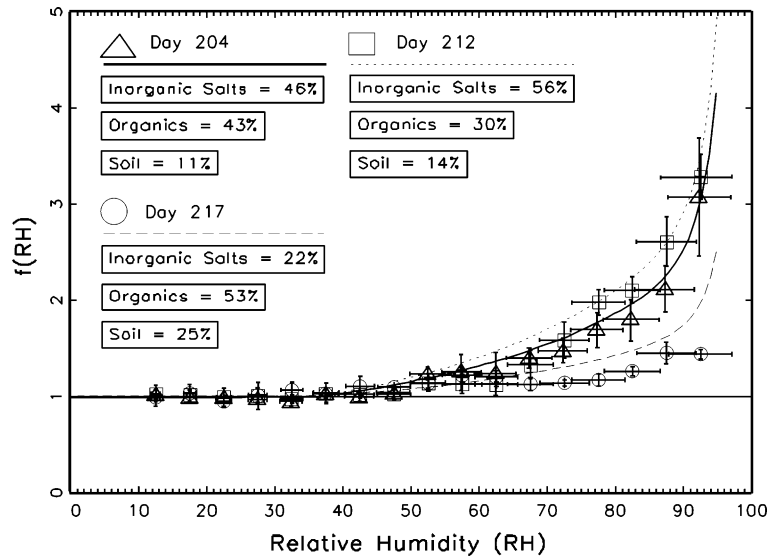


Fig. 3. Plot of measured $f(\text{RH})$ values for Julian days 207, 211 and 224 at Great Smoky. Measured data are presented as points with uncertainty bars. The uncertainty bars represent a $\pm 5\%$ uncertainty for measured relative humidity, while the uncertainty bars for $f(\text{RH})$ represent the measurement uncertainty of the integrating nephelometers. The lines are the result of a curve fit through the data points. The percent composition of the major aerosol species is also presented for each day.

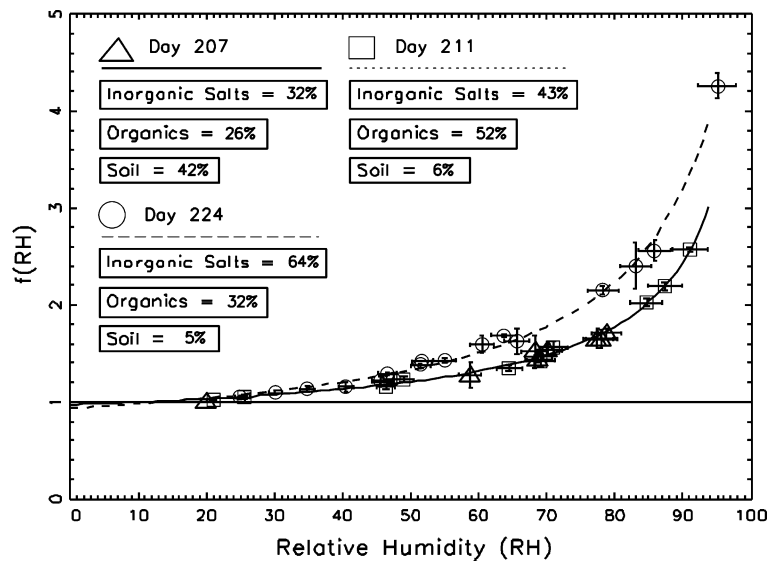


Fig. 4. Plot of measured $f(\text{RH})$ values for Julian days 204, 212 and 217 at Grand Canyon. Measured data are presented as points with uncertainty bars. The uncertainty bars represent a $\pm 5\%$ uncertainty for measured relative humidity, while the uncertainty bars for $f(\text{RH})$ represent one standard deviation of all measurements made within one 5% relative humidity range. The lines through the data points are the result of theoretical estimates of $f(\text{RH})$. The percent composition of the major aerosol species is also presented for each day.

relative humidity range of 63–67%, 80% of the aerosols did not split into two growth regimes and that above 73%, most TDMA measurements indicate a deliquescent point where two aerosol growth fractions are observed.

Our measurements indicate that on about 45% of the days, there is some growth below about 67% relative humidity, typically starting in the 35–45% RH range, but at about 67% RH, a deliquescent point is observed.

Julian days 204 and 212, correspond to hygroscopic inorganic (sulfates plus nitrates) fractions of 56% and 46%, respectively, these days should be contrasted with Julian day 217 where the 24 h average inorganic hygroscopic fraction was only 22%. Julian day 217 was associated with smoke from a forest fire on the north rim of the Grand Canyon. The measured ambient extinction and scattering showed short-term variability throughout the day and therefore the 24 h aerosol measurement is unlikely to be representative of the time the $f(\text{RH})$ curve was measured. In fact, the $f(\text{RH})$ curve for Julian day 217 does not show a continuous increase in $f(\text{RH})$ over the whole relative humidity range. $f(\text{RH})$ increases from 40% to 57% relative humidity and then is suppressed somewhat with less increase in the 65–80% range.

Fig. 4 shows a similar plot for the Great Smoky data set. On Julian days 207, 211 and 224 the hygroscopic inorganic fractions were 32.6%, 42.7%, and 63.5%, respectively. The higher the fraction content of inorganic hygroscopic material the greater the increase in $f(\text{RH})$ as a function of relative humidity. The solid lines in these curves represent a curve fit to the observed data. (Day et al., 2000). Displays of all individual $f(\text{RH})$ curves did not show evidence for deliquescence.

Referring to Tables 3 and 4, the mean $f(\text{RH})$ in the 20–25% relative humidity range at Great Smoky was 1.06, while at Grand Canyon it was 1.0; in the 35–40% relative humidity range the $f(\text{RH})$ was 1.21, at Great Smoky, while at Grand Canyon it was only 1.05. In the higher relative humidity ranges, the Great Smoky $f(\text{RH})$ values always exceeded those of Grand Canyon but by smaller fractional amounts.

6. Comparison of measured $f(\text{RH})$ with theoretical predictions

Malm et al. (2000) report on a comparison between measured and modeled $b_{\text{scat}}(\text{RH})/b_{\text{scat,dry}}$ ratios for the Great Smoky data set. Models, described in the section on *Comparison between estimated and measured scattering at Great Smoky Mountains National Park*, used for the comparison were external with constant mass scattering but with sulfate ammoniation and associated growth accounted for, external with sulfate size, ammoniation, and growth incorporated, and the mixed model. In most cases, all three modeling approaches agreed well with each other, however, the ratios predicted by the mixed and external models at times differed from each other under high relative humidity conditions by as much as 30%, with the mixed model showing less increase in scattering than the external models.

Measured ratios, in general, were well reproduced by all of the modeling approaches. The R^2 between measured and modeled ratios varied from 0.92 to 0.71, with the external models having the highest R^2 . All models,

under higher relative humidity conditions, yielded ratios that were on the average greater than those that were measured. The largest discrepancies occurred when organic mass concentrations were highest with modeled ratios being greater than those measured.

Table 3 summarizes the differences between measured and calculated $f(\text{RH})$ values for successive RH intervals of 5%. An externally mixed aerosol model, which accounts for ammoniation and particle size, assumes organics are nonhygroscopic, and uses sulfate growth curves that were smoothed between the deliquescent and crystallization points was used for estimating $f(\text{RH})$ values. Table 3 shows that there is some bias between measured and predicted $f(\text{RH})$ values in that $f(\text{RH})$, and thereby growth, is under predicted at lower RH values (by about 10%) but over predicted above about 65% RH. However, the overall agreement, given the assumptions concerning growth between the crystallization and deliquescent points, between measured and predicted $f(\text{RH})$, is remarkable. The R^2 , associated with an OLS regression between the variables is 0.92.

Comparisons between modeled and measured $b_{\text{scat}}(\text{RH})/b_{\text{scat,dry}}$ ratios have not been previously reported for the Grand Canyon data set and will therefore, be presented here. Because little difference is observed between the mixed and external models and because particle size measurements were not carried out, only the external model with constant mass scattering coefficients will be considered. Consistent with the discussions above and Malm and Day (2000) the following equation is used to estimate scattering as a function of relative humidity:

$$b_{\text{scat}} = (2.2)f(\text{RH}) [\text{SULFATE} + \text{NITRATE}] + (1.8)f_{\text{org}}(\text{RH})[\text{OMC}] + (1)[\text{SOIL}], \quad (4)$$

where b_{scat} is the scattering coefficient, [SULFATE] is the SO_4 ion mass concentration adjusted to ammonium sulfate; [NITRATE], [OMC], and [SOIL] are the concentrations of ammonium nitrate, organic carbon, and soil, respectively. The coefficient numbers refer to the assumed dry mass scattering efficiencies of the respective species in units of $\text{m}^2 \text{gm}^{-1}$. The $f(\text{RH})$ is the scattering enhancement factor for sulfates and nitrates, $f_{\text{org}}(\text{RH})$ refers to organics. The function, $f(\text{RH})$, was calculated on a sampling-period-by-sampling-period basis using Tang's ammonium sulfate D/D_0 curves. Estimates of $f(\text{RH})$ are based on growth curves that were smoothed between the crystallization and deliquescent points and on a lognormal sulfate species mass size distribution with a geometric mass mean diameter of $0.2 \mu\text{m}$ and a geometric standard deviation, σ_g , of 2.3. These size parameters are consistent with previous measurements of sulfate mass size distribution (Malm and Pitchford, 1997). The $f(\text{RH})$ associated with nitrates was assumed to be the same as for sulfates, while $f_{\text{org}}(\text{RH})$ for organics was set equal to one.

Fig. 3 shows the theoretical calculation of the growth curves as solid and dashed lines, while the data points with associated error bars are measured values. On Julian day 204, measured and predicted estimates compare quite favorably and the smoothing scheme on the average works quite well. However, even though the predictions tend to be within the error bars associated with the measurements, the predicted values tend to be somewhat higher than measured in the 60–80% RH range, while below the deliquescent point of about 50% the predicted values are greater than measured. However, on Julian day 212, growth assumptions result in a significant over prediction of scattering in the 50–75% relative humidity range. There were a number of sampling periods where the estimated $f(\text{RH})$ curves were overestimated in this same relative humidity region. Conversely, on 4 out of the 32 sampling days where predicted and measured values could be compared, measured $f(\text{RH})$ values were between 15% and 25% greater than predicted in the 80–90% RH range. Measured and predicted values can be made to agree on these days by adjusting growth parameters associated with sulfates and nitrates, adjusting dry mass scattering efficiencies in Eq. (4) from their nominal values or assume that the $f(\text{RH})_{\text{org}}$ is greater than one. Based on our data we cannot rule out any of these possibilities.

It is of interest to point out that Pitchford and McMurry (1994) observed that on 2 of 8 sampling days at Grand Canyon, particle growth, as measured by a TDMA, assuming only the inorganic species to be hygroscopic, under predicted water uptake by about 30%. Saxena et al. (1995) using this same data set suggest that on these two days organics are responsible for the extra growth. However, it is further pointed out by Pitchford and McMurry (1994) that if the volume fraction of the inorganic soluble components during the few hours of TDMA growth measurements were $0.6 \mu\text{g m}^{-3}$ instead of about $0.4 \mu\text{g m}^{-3}$ as estimated from the 24-h averaged MOUDI measurements, the measured growth would be consistent with growth associated only with the inorganic soluble fraction.

The differences between measured and estimated $f(\text{RH})$ values for different relative humidity regions is summarized in Table 4. The average of all measured $f(\text{RH})$ values within a specified relative humidity range compare favorably to theoretically predicted values, however, the agreement is slightly better at low and high relative humidities than at mid-range humidities. At low relative humidities, measured $f(\text{RH})$ shows growth starting as low as 25% RH and increasing slowly to 1.05 at the 35–40% RH range, while the theoretical calculations show zero growth or no change from one in this same range.

An ordinary least-squares (OLS) regression between measured and predicted $f(\text{RH})$ values yields an $R^2 = 0.82$ with slope of 1.02 ± 0.006 when the intercept

term is forced through zero. The implication is that, on the average, predicted $f(\text{RH})$ values are about 2% greater than measured.

7. Statistical estimates of $b_{\text{scat}}(\text{RH})/b_{\text{scat,dry}}$

The amount of scattering at a specific relative humidity can be estimated using

$$b_{\text{scat,water}}(\text{RH}) = a_0 + a_1[\text{SULFATE}] + a_2[\text{OMC}] + \dots + a_n[\text{Other Species}], \quad (5)$$

where $b_{\text{scat,water}}(\text{RH})$ is scattering due to water at some RH, $a_1 = e_s[f(\text{RH})_s - 1]$, $a_2 = e_{\text{oc}}[f(\text{RH})_{\text{oc}} - 1]$ and so forth, a_0 is interpreted as scattering associated with residual water, e_s and e_{oc} are the average dry mass scattering coefficients associated with sulfates and organics, respectively. $b_{\text{scat,water}}(\text{RH}) = b_{\text{scat}}(\text{RH}) - b_{\text{scat,dry}}$ is calculated on a sampling-period-by-sampling-period basis by estimating $b_{\text{scat}}(\text{RH})$ using measured $b_{\text{scat}}(\text{RH})/b_{\text{scat,dry}}$ ratios and then differencing scattering at some RH and dry scattering. Eq. (5) can then be solved at specific humidities using OLS regressions with or without an intercept.

For the Great Smoky data set, the coefficients for sulfate are highly significant for all relative humidities for both the intercept and nonintercept regressions. The coefficient associated with organics is significant at better than the 5% level for humidities greater than 50% for the zero intercept model and greater than 25% for the non-zero model. Regression coefficients associated with other species were not statistically significant. R^2 s varied from a low of 0.89 to a high of 0.98.

Fig. 5 is a plot of the $f(\text{RH})$ curves derived from the OLS analysis with an intercept term assuming $e_s = 2.4 \pm 0.5 \text{ m}^2 \text{ gm}^{-1}$ and $e_{\text{oc}} = 4.0 \text{ m}^2 \text{ gm}^{-1}$. The error bars represent the standard error of the regression coefficients, while the rectangle enclosing each error bar is associated with the standard deviation of the theoretically calculated dry scattering coefficients ($\pm 0.5 \text{ m}^2 \text{ gm}^{-1}$) that are based on measured sulfate size distributions (Malm et al., 2000). The solid and dashed lines are the theoretically calculated $f(\text{RH})$ curves for ammonium bisulfate and sulfuric acid, respectively, assuming $D_g = 0.36 \mu\text{m}$ and $\sigma_g = 1.92$ (Malm et al., 2000). The average ammonium-to-sulfate molar ratio for the study was near one, however, on the higher sulfate days the molar ratio tended toward values less than one, while on lower sulfate concentration days the sulfate aerosols were more neutralized. It is the higher mass concentrations that tend to influence the regression coefficients most and, therefore, the statistically derived $f(\text{RH})$ curve is somewhat greater than the ammonium bisulfate curve but significantly less than the sulfuric acid $f(\text{RH})$ curve.

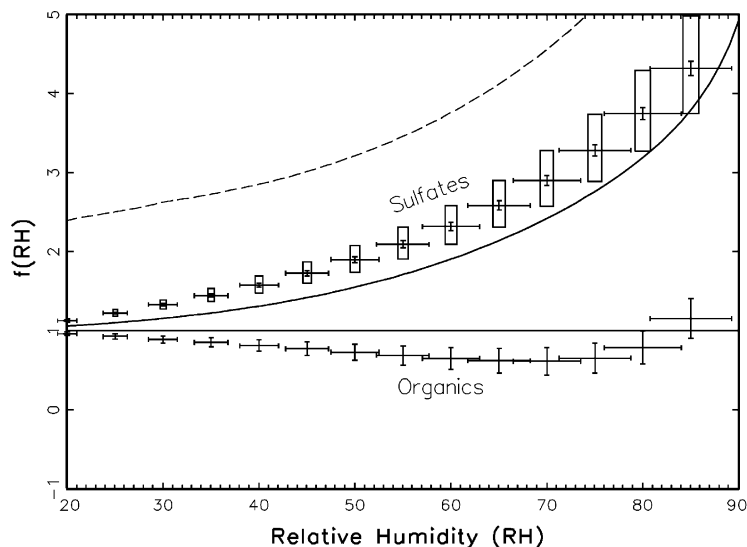


Fig. 5. $f(\text{RH})$ is plotted as the solid and broken line for ammonium bisulfate and sulfuric acid, respectively, while the single data points with error bars show the OLS regression with an intercept derived $f(\text{RH})$ for sulfates and organics. The error bars correspond to the standard errors of the regression coefficients, while the upper and lower edges of the rectangle represent the $f(\text{RH})$ that corresponds to \pm one standard deviation of dry mass scattering efficiency that was calculated from measured size distributions.

An interesting feature of the regressions is the highly significant negative regression coefficients associated with organics. The implication of a negative regression coefficient is reflected in the organic $f(\text{RH})$ curves shown in Fig. 5. An $f(\text{RH})$ curve less than one implies that organics would be less efficient at scattering light than predicted by an equation of the type given in Eq. (2), or that the effect of organics is to reduce the ability of sulfates in a sulfate organic mixture to absorb water and thereby reduce the specific scattering efficiency of the mixture. Although the organic $f(\text{RH})$ curve is slightly less than one at all relative humidities $f(\text{RH}) \pm$ standard error, for the most part, overlaps one. Therefore, any interpretation concerning organic suppression of water absorption should be considered speculative.

The intercept term is identified as residual or unaccounted for water scattering and varies from about 0.6 Mm^{-1} at 20% RH to 2.82 Mm^{-1} at 65% RH. Because dry scattering was measured at about 15% RH and because nitrates were not included in the regression analysis, some residual water scattering can be expected. Theoretical estimates of average nitrate scattering vary from about 0.04 Mm^{-1} at 20% RH to 2.0 Mm^{-1} at 85% RH, while the average sulfate scattering at 15% RH is estimated to be 1.8 Mm^{-1} . Therefore, an intercept term on the order of $2\text{--}3 \text{ Mm}^{-1}$ is consistent with expected residual water scattering.

Both the theoretical calculations of measured $f(\text{RH})$ curves and the statistical determination of the average $f(\text{RH})$ function associated with each species suggests that

organics do not uptake water in a significant way. On the other hand, Dick et al. (2000) report on modeled growth using TDMA data collected during the same field study and present convincing evidence that organics are responsible for some water absorption. However, there are some basic differences in our respective assumptions. Whereas we assumed, for purposes of model calculations and have shown with the statistical analysis, that smoothing between the deliquescent and crystallization branches may be a valid assumption concerning sulfate growth, they made an argument, that sulfate deliquesces and therefore assumes the deliquescent branch of the measured growth curves. Any growth not accounted for below the deliquescent points was interpreted as growth due to organic absorption of water. However, if it assumed that the overall growth curve is continuous, this assumption implies that organics grow more in the relative humidity ranges below the sulfate deliquescent point than above and because sulfates grow in a stepwise manner at the deliquescent points, organics have a commensurate stepwise decrease in growth at those sulfate deliquescent relative humidities. Organic growth of this nature seems to be unrealistic.

For the most part a cursory examination of their plots of measured and predicted growth for the $0.2 \mu\text{m}$ particles, suggest that an assumption of “smoothed” growth curves would result in a favorable comparison assuming only inorganic hygroscopicity at least for the time periods presented in their paper. Furthermore in their conclusions they state that “the most accurate model of

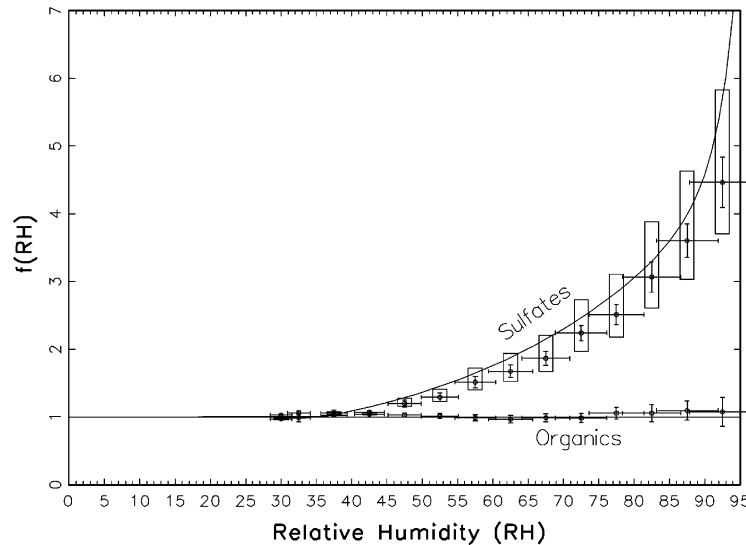


Fig. 6. $f(\text{RH})$ is plotted as the solid line for ammonium sulfate, while the single data points with error bars show the OLS regression with an intercept derived $f(\text{RH})$ for sulfates and organics. The error bars correspond to the standard errors of the regression coefficients, while the upper and lower edges of the rectangle represent the $f(\text{RH})$ that corresponds to \pm one standard deviation of dry mass scattering efficiency that was calculated from measured size distributions.

water content for aerosols sampled at ambient conditions during moderate to high relative humidity may be obtained by adding organic-attributable water to supersaturated sulfate water” as opposed to using the deliquescent branch as they did in their paper.

Another significant difference between the TDMA and $b_{\text{scat}}(\text{RH})/b_{\text{scat,dry}}$ data is that the scattering measurements are a result of integrating the scattered light by all particles less than $2.5\ \mu\text{m}$ while the data presented in Dick et al. (2000) focuses on particles less than $0.4\ \mu\text{m}$ particles and primarily on $0.2\ \mu\text{m}$. It is possible the smaller organic size fractions (those that are less optically active the $530\ \text{nm}$ wavelength of the nephelometer) are more hygroscopic than larger particles and therefore the nephelometer would not be sensitive to their growth.

Fig. 6 is for the Grand Canyon data set and is similar to Fig. 5. The sulfate regression coefficient is significant at less than 1% at all humidities greater than 40%, while the regression coefficient associated with all other species are not statistically significant. Moreover, the intercept term is not statistically different from zero. The R^2 s varied between 0.6 and 0.75. As before, the error bars represent the standard error of the regression coefficients, while the rectangle enclosing each error bar represents the standard deviation of theoretically calculated dry scattering coefficients ($2.2 \pm 0.65\ \text{m}^2\ \text{gm}^{-1}$) that were based on measured sulfate size distributions (Malm and Pitchford, 1997). Even though the organic regression coefficients were not statistically significant, the implied

organic $f(\text{RH})$ curve is included for reference. Notice that the average $f(\text{RH})$ data points shown in Fig. 6 reflects a deliquescence at about 45% relative humidity, however the second deliquescent point that occurred in the 60–70% range on some of the sampling days is not reflected on the average. The solid line corresponds to the theoretically derived ammonium sulfate $f(\text{RH})$ curve used in Eq. (4). This $f(\text{RH})$ curve, which is based on ammonium sulfate growth curves that have been smoothed between the deliquescent and crystallization points, approximates the statistically derived growth curve quite well.

8. Conclusions

Understanding of the hygroscopic properties of ambient aerosols as they relate to visibility impairment was in part the motivation for the two studies reported on in this paper. The Great Smoky study was carried out from 15 July 1995 through 25 August 1995, while the Grand Canyon study was conducted from 10 July 1998 through 8 August 1998 on the south rim of the Grand Canyon. Scattering as a function of relative humidity was measured with a humidograph allowing for estimates of $f(\text{RH}) = b_{\text{scat(wet)}}/b_{\text{scat(dry)}}$, which is used to develop a better understanding of aerosol growth. Modeling scattering as a function of relative humidity serves to both explore the validity of aerosol growth and mixing models and associated assumptions, and provide an estimate of the

hygroscopicity of aerosol species other than sulfates and nitrates.

The $f(\text{RH})$ function was smoothly increasing as a function of increasing relative humidity at Great Smoky while at Grand Canyon on about 45% of the sampling days particles deliquesced in the 25–55% relative humidity range and on those days a second discontinuity in growth was observed in the 60–70% relative humidity range. Furthermore, at Grand Canyon, the $f(\text{RH})$ was more varied than at Great Smoky. For instance, in the range of 80–85% relative humidity the $f(\text{RH})$ values varied between 1.53 and 2.75 at Great Smoky, while at Grand Canyon the range was from near 1 to 4.0. Part of the explanation of these differences is that in the eastern United States sulfates make up a large fraction of fine mass, while in the West sulfates plus nitrates can actually be a small fraction of fine mass, with organics and soil dust being the major contributors. In general, as organics and soil dust increase the rate of increase of $f(\text{RH})$ with humidity decreases.

A variety of scattering models were used to estimate measured $f(\text{RH})$ curves. At Great Smoky, an externally mixed aerosol model was assumed with and without sulfate ammoniation, and with and without accounting for sampling-period-to-sampling-period shifts in size distribution. These same variations were explored assuming a mixed aerosol model. The sensitivity to using the deliquescent and crystallization branches as well as a curve smoothed between the deliquescent and crystallization points of the sulfate D/D_0 curves as a function of relative humidity was also explored. Accounting for aerosol growth as a function of sulfate ammoniation and using the smoothed D/D_0 growth curves were the two assumptions that were most important in achieving a theoretical prediction of measured $f(\text{RH})$ curves. Assuming either the deliquescent or crystallization branch of the sulfate hysteresis curve would have either under or over predicted $f(\text{RH})$ in the hysteresis relative humidity region.

Accounting for sulfate mass size distribution on a sampling period by sampling period bases made only marginal improvements in the ability of models to predict measured $f(\text{RH})$ as did assumptions concerning aerosol mixing. Differences between the externally and internally mixed models were less than 10% on the average.

At Grand Canyon, only the external model was used; sulfate was assumed to be in the form of ammonium sulfate and a smoothed $f(\text{RH})$ curve was used based on size distribution measurements made in previous studies. An OLS regression between measured and predicted $f(\text{RH})$ values yields a $R^2 = 0.82$ with a slope of 1.02 ± 0.006 when the intercept term is forced through zero. The implication being that on the average predicted $f(\text{RH})$ values are about 2% greater than measured.

Finally, a model was developed to estimate the $f(\text{RH})$ function associated with individual aerosol species. Assuming dry mass scattering coefficients, scattering due to absorbed aerosol water relates to aerosol species concentrations in a linear way at a given relative humidity.

The regression coefficients, resulting from regressing measured scattering attributable to aerosol water against aerosol mass concentrations, are functions of dry mass scattering efficiency and $f(\text{RH}) = b_{\text{scat}}(\text{RH})/b_{\text{scat,dry}}$ at a specified relative humidity. The resulting $f(\text{RH})$ curve that is associated with a given data set is interpreted as an average $f(\text{RH})$ for the time period corresponding to that data set. It is emphasized that the resulting $f(\text{RH})$ curves are, except for the assumed dry mass scattering coefficients, based solely on measured data. Assumptions concerning the hysteresis characteristics of the aerosol growth curves or on the fraction of organics or any other species that may or may not be hygroscopic are not required.

At Great Smoky, the measured $f(\text{RH})$ was on the average slightly greater than the average theoretical curve for ammonium bisulfate implying slightly more growth than would have been predicted from the measured ammoniation (average molar ratio of ammonium to sulfate was one) and size parameters. At Grand Canyon, the measured $f(\text{RH})$ curve was slightly less than the estimated $f(\text{RH})$ curve based on the assumption of full sulfate neutralization.

For both data sets, the assumptions concerning smoothing of the sulfate hysteresis curves between the deliquescent and crystallization branches of the sulfate hysteresis curves appears to be a reasonable approximation of actual growth and, within the statistical uncertainty of the regression analysis, organics are judged to be weakly to nonhygroscopic. In fact, for the Great Smoky data set the analysis suggests that organics may have suppressed the ability of sulfates to absorb water.

Disclaimer

The assumptions, findings, conclusions, judgements, and views presented herein are those of the authors and should not be interpreted as necessarily representing official National Park Service policies.

Acknowledgements

The authors would like to thank Dr. Sonia Kreidenweis of Colorado State University for helpful discussions in regards to this paper. We would also like to acknowledge Air Resource Specialists, Inc. and University of California, Davis for their support in various aspects of this field research.

References

- Blando, J.D., Porcia, R.J., Li, T.H., Bowman, D., Lioy, P.J., Turpin, B.J., 1998. Secondary formation and the Smoky Mountain organic aerosol: an examination of aerosol polarity and functional group composition during SEAVS. *Environment Science and Technology* 32, 604–613.
- Cahill, T.A., Goodart, C., Nelson, J.W., Eldred, R.A., Nastro, J.S., Feeney, P.J., 1985. Design and evaluation of the DRUM impactor. In: Airman, T., Veziroglu, T.N. (Eds.), *International Symposium on Particulate and Multi-phase Processes*. Hemisphere Publishing Corporation, Washington, DC, pp. 319–325.
- Cai, X., Turpin, B.J., McMurry, P.H., 1993. Particle growth as a function of size and humidity (TDMA), in 1992 Measurements of Aerosol Composition and Optics in Meadview, AZ (in conjunction with Project MOHAVE). Report on Project RP2023-11 to Electric Power Research Institute (EPRI), Palo Alto, California, University of Minneapolis, Minneapolis.
- Chan, T., Lippman, M., 1977. Particle collection efficiencies of air sampling cyclones: an empirical theory. *Environmental Science and Technology* 11, 377–382.
- Chow, J.C., Watson, J.G., Pritchell, L.C., Pierson, W.R., Frazier, C.A., Purcell, R.G., 1993. The DRI thermal/optical reflectance carbon analysis system: description, evaluation and applications in US air quality studies. *Atmospheric Environment* 27A, 1185–1201.
- Chughtai, A.R., Williams, G.R., Atteya, M.M.O., Miller, N.J., Smith, D.M., 1999. Carbonaceous particle hydration. *Atmospheric Environment* 33, 2679–2687.
- Covert, D.S., Waggoner, A.P., Weiss, R.E., Ahlquist, N.C., Charlson, R.J., 1979. Atmospheric aerosols, humidity and visibility. In: *Character and Origins of Smog Aerosols*. Wiley, New York, pp. 559–581.
- Day, D.E., Malm, W.C., Kreidenweis, S.M., 1997. Aerosol light scattering measurements: a comparison of differently configured optec nephelometers. In: *Visual Air Quality: Aerosols and Global Radiation Balance*. In: *Proceedings of a Specialty Conference Sponsored by Air and Waste Management Association and Geophysical Union*, Barlett, New Hampshire, September 9–12, pp. 952–96.
- Day, D.E., Malm, W.C., Kreidenweis, S.M., 2000. Aerosol light scattering measurements as a function of relative humidity. *Journal of the Air and Waste Management Association* 50, 710–716.
- Decesari, S., Facchini, M.C., Fuzzi, S., Tagliavini, E., 2000. Characterization of water-soluble organic compounds in atmospheric aerosol: a new approach. *Journal of Geophysical Research* 105, 1481–1489.
- Dick, W.D., Saxena, P., McMurry, P.H., 2000. Estimation of water uptake by organic compounds in submicron aerosols measured during the Southeastern aerosol and visibility study. *Journal of Geophysical Research* 105, 1471–1479.
- Malm, W.C., Day, D.E., 2000. Optical properties of aerosols at Grand Canyon National Park. *Atmospheric Environment* 34, 3373–3391.
- Malm, W.C., Day, D.E., Kreidenweis, S.M., 2000. Light scattering characteristics of aerosols as a function of relative humidity: Part I—comparison of measured scattering and aerosol concentrations using the theoretical models. *Journal of the Air and Waste Management Association* 50, 686–700.
- Malm, W.C., Pitchford, M.L., 1997. Comparison of calculated sulfate scattering efficiencies as estimated from size-resolved particle measurements at three national locations. *Atmospheric Environment* 31, 1315–1325.
- Malm, W.C., Sisler, J.F., Huffman, D., Eldred, R.A., Cahill, T.A., 1994. Spatial and seasonal trends in particle concentration and optical extinction in the United States. *Journal of Geophysical Research* 99, 1347–1370.
- Marple, V.A., Rubow, K.L., Behm, S.M., 1991. A microorifice uniform deposit impactor (MOUDI): description, calibration, and use. *Aerosol Science and Technology* 14, 434.
- McDow, S.R., Vartianen, M., Sun, Q., Hong, Y., Yao, Y., Kamens, R.M., 1994. Combustion aerosol water content and its effect on polycyclic aromatic hydrocarbon reactivity. *Atmospheric Environment* 29, 791–797.
- McMurry, P.H., Zhang, X., 1991. Optical Properties of Los Angeles aerosols: an analysis of data acquired during SCAQS. Final Report on Project SCAQS-5–8 to the Coordinating Research Council, Atlanta Georgia, University of Minneapolis, Minneapolis.
- Molenaar, J.V., 1997. Analysis of the real world performance of the Optec NGN-2 ambient nephelometer. In: *Visual Air Quality: Aerosols and Global Radiation Balance*, Proceedings of a Speciality Conference Sponsored by Air and Waste Management Association and Geophysical Union, Barlett, New Hampshire, September 9–12, pp. 243–265.
- Pilinis, C., Seinfeld, J.H., 1987. Continued development of a general equilibrium model for inorganic multicomponent atmospheric aerosols. *Atmospheric Environment* 21, 2453–2466.
- Pitchford, M.L., McMurry, P.H., 1994. Relationship between measured water vapor growth and chemistry of atmospheric aerosol for Grand Canyon, Arizona, in winter 1990. *Atmospheric Environment* 28, 827–839.
- Quinn, P.K., Coffman, D.J., 1998. Local closure during the first aerosol characterization experiment (ACE 1): aerosol mass concentration and scattering and backscattering coefficients. *Journal of Geophysical Research* 103, 16575–16596.
- Raabe, O.G., Braaten, D.A., Axelbaum, R.L., Teague, S.V., Cahill, T.A., 1988. Calibration studies of the DRUM impactor. *Journal of Aerosol Science* 19, 183–195.
- Rogge, W.F., Mazurek, M.A., Hildemann, L.M., Cass, G.R., 1993. Quantification of urban organic aerosols at a molecular level: identification, abundance and seasonal variation. *Atmospheric Environment* 27A, 1309–1330.
- Saxena, P., Hildemann, L.M., 1996. Water-soluble organics in atmospheric particles: a critical review of the literature and application of thermodynamics to identify candidate compounds. *Journal of Atmospheric Chemistry* 24, 57–109.
- Saxena, P., Hildemann, L.M., McMurry, P.H., Seinfeld, J.H., 1995. Organics alter hygroscopic behavior of atmospheric particles. *Journal of Geophysical Research* 100, 18755–18770.
- Stelson, A.W., Seinfeld, J.H., 1982. Thermodynamic prediction of the water activity, NH_4NO_3 dissociation constant, density and refractive index for the NH_4NO_3 – $(\text{NH}_4)_2\text{SO}_4$ – H_2O system at 25°C. *Atmospheric Environment* 16, 2507–2514.
- Tang, I.N., 1997. Thermodynamic and optical properties of mixed-salt aerosols of atmospheric importance. *Journal of Geophysical Research* 102, 1883–1893.

- Tang, I.N., 1976. Phase transformations and growth of aerosol particles composed of mixed salts. *Journal of Aerosol Science* 7, 361–371.
- Tang, I.N., Munkelwitz, H.R., 1994. Water activities, densities, and refractive indices of aqueous sulfates and sodium nitrate droplets of atmospheric importance. *Geophysical Research* 99, 18801–18808.
- Tang, I.N., Munkelwitz, H.R., 1991. Composition and temperature dependence of the deliquescence properties of hygroscopic aerosols. *Atmospheric Environment* 27A, 467–473.
- Trijonis, J.C., Malm, W.C., Pitchford, M., White, W.H., Charlson, R., Husar, R., 1990. Visibility: existing and historical conditions-causes and effects, State Science and State Technology Report 24. National Acid Precipitation Assessment Program, Washington, DC.
- Waggoner, A.P., Weiss, R.E., Larson, T.V., 1983. In-situ rapid response measurement of $\text{H}_2\text{SO}_4/(\text{NH}_4)_2\text{SO}_4$ aerosols in urban Houston: a comparison with rural Virginia. *Atmospheric Environment* 17, 1723–1731.
- Watson, J.G., Chow, J.C., Richards, L.W., Neff, W.D., Andersen, S.R., Dietrich, D.L., Olmez, I., 1988. The 1987–88 Denver brown cloud study. Desert Research Institute Report 8810, 1F2, Desert Research Institute, Reno, NV.
- Wexler, A.S., Seinfeld, J.H., 1991. Second-generation inorganic aerosol model. *Atmospheric Environment* 25A, 2731–2748.
- Zhang, X.Q., Turpin, B.J., McMurry, P.H., Hering, S.V., Stolzenburg, M.R., 1994. Mie theory evaluation of species contributions to 1990 wintertime visibility reduction in the Grand Canyon. *Journal of the Air and Waste Management Association* 44, 153–162.
- Zhang, X.Q., McMurry, P.H., Hering, S.V., Casuccio, G.S., 1993. Mixing characteristics and water content of submicron aerosols measured in Los Angeles and at the Grand Canyon. *Atmospheric Environment* 27A, 1593–1607.
- Zhang, X.Q., McMurry, P.H., 1992. Evaporation losses of fine particulate nitrates during sampling. *Atmospheric Environment* 26A, 3305–3312.